The Plant Cell, Vol. 22: 3423–3438, October 2010, www.plantcell.org

The Cytoskeleton and the Peroxisomal-Targeted SNOWY COTYLEDON3 Protein Are Required for Chloroplast Development in *Arabidopsis* [W]

Verónica Albrecht,[a,1] Klára Šimková,[b] Chris Carrie,[c] Etienne Delannoy,[c] Estelle Giraud,[c] Jim Whelan,[c] Ian David Small,[c] Klaus Apel,[b,2] Murray R. Badger,[a] and Barry James Pogson[a]

[a] ARC Centre of Excellence in Plant Energy Biology, Research School of Biology, Australian National University Canberra, Acton, Australian Capital Territory 0200, Australia

[b] Institute of Plant Sciences, ETH Zurich, 8092 Zurich, Switzerland

[c] ARC Centre of Excellence in Plant Energy Biology, University of Western Australia, Crawley, Western Australia 6009, Australia

Here, we describe the *snowy cotyledon3* (*sco3-1*) mutation, which impairs chloroplast and etioplast development in *Arabidopsis thaliana* seedlings. SCO3 is a member of a largely uncharacterized protein family unique to the plant kingdom. The *sco3-1* mutation alters chloroplast morphology and development, reduces chlorophyll accumulation, impairs thylakoid formation and photosynthesis in seedlings, and results in photoinhibition under extreme CO_2 concentrations in mature leaves. There are no readily apparent changes to chloroplast biology, such as transcription or assembly that explain the disruption to chloroplast biogenesis. Indeed, SCO3 is actually targeted to another organelle, specifically to the periphery of peroxisomes. However, impaired chloroplast development cannot be attributed to perturbed peroxisomal metabolic processes involving germination, fatty acid β-oxidation or photorespiration, though there are so far undescribed changes in low and high CO_2 sensitivity in seedlings and young true leaves. Many of the chloroplasts are bilobed, and some have persistent membranous extensions that encircle other cellular components. Significantly, there are changes to the cytoskeleton in *sco3-1*, and microtubule inhibitors have similar effects on chloroplast biogenesis as *sco3-1* does. The localization of SCO3 to the periphery of the peroxisomes was shown to be dependent on a functional microtubule cytoskeleton. Therefore, the microtubule and peroxisome-associated SCO3 protein is required for chloroplast development, and *sco3-1*, along with microtubule inhibitors, demonstrates an unexpected role for the cytoskeleton and peroxisomes in chloroplast biogenesis.

INTRODUCTION

The development of a photosynthetically competent chloroplast requires the coordinated synthesis, targeting, and assembly of thousands of proteins, metabolites, and pigments. The functions of chloroplasts extend beyond photosynthesis to the biosynthesis of amino acids, hormones, lipids, sugars, and starch. Consequently, energy metabolism by the other two energy organelles, mitochondria and peroxisomes, are interdependent with some processes within the chloroplasts. This would suggest a requirement for coordinated biogenesis; yet research to date has focused on communication from plastids to the nucleus to coordinate gene expression, a process termed chloroplast retrograde signaling (Pogson et al., 2008). This has been presumed to be direct communication, not involving other cellular compartments such as the cytoskeleton or peroxisome. A new aspect to the discussion about chloroplast function arose recently with the inclusion of stromules, mobile and transitory chloroplast structures that have been shown to transmit proteins from one chloroplast to another and to encircle other organelles (Reski, 2009). Stromules are highly mobile, transient membranous extensions of plastids thought to function in interorganelle exchange of metabolites, but as they are transient and rare in green tissues, studying them has proved difficult (Gunning, 2005; Natesan et al., 2005).

Disruptions of chloroplast function, such as impaired chloroplast protein import in mutations of the translocon of the outer and the inner envelope of chloroplasts, the TOC/TIC complex, like *toc159*, *toc33*, and *toc34* (Asano et al., 2004; Gutensohn et al., 2004), lead to white or pale-green plants that often are not able to survive on soil. Other mutations involved in protein modification or integration into the membrane systems, such as *CHAPERONIN 60* (*schlepperless*) and plastid peptidases (*plsp1*), result in embryo-lethal or albino mutant seedlings (Apuya et al., 2001; Inoue et al., 2005). Also, tight regulation of chloroplast protein biosynthesis and protein degradation, such as in the assembly of photosystem II (PSII), has been shown to be important for development of functional chloroplasts in the true leaves of the *variegated2* (*var2*) mutant (Miura

[1] Address correspondence to veronica.albrecht@anu.edu.au.

[2] Current address: Boyce Thompson Institute for Plant Research, Ithaca, NY 144853-1801.

The author responsible for distribution of materials integral to the findings presented in this article in accordance with the policy described in the Instructions for Authors (www.plantcell.org) is: Verónica Albrecht (veronica.albrecht@anu.edu.au).

[W] Online version contains Web-only data.

www.plantcell.org/cgi/doi/10.1105/tpc.110.074781

et al., 2007). These are just a few examples showing that the knockout of proteins required for chloroplast function results in severe phenotypes, such as embryo lethality, albinism, or pale-green plants.

Severe functional impairment or bleaching of chloroplasts normally results in a reduction in expression of nuclear genes required for photosynthesis (Surpin et al., 2002). This down-regulation requires a retrograde signal from the chloroplast, which has been shown to be disrupted by *genomes uncoupled* (*gun*) mutations. *GUN1* encodes a pentatricopeptide repeat protein, while other *GUN* genes encode enzymes or regulatory factors involved in tetrapyrrole biosynthesis, including GUN4 and GUN5 (Vinti et al., 2000; Koussevitzky et al., 2007).

A degree of complexity to consider is that chloroplast development differs between the embryonic leaves called cotyledons and so-called true leaves derived from the apical meristem. Chloroplast biogenesis in cotyledons is the result of coordinated synthesis of proteins, lipids, and metabolites commencing in a progenitor organelle called a proplastid, either directly forming a chloroplast or via the intermediate state called an etioplast (Lopez-Juez and Pyke, 2005). Proplastids are relatively small, undifferentiated, and of an irregular globular structure with vesicles. Proplastids differentiate in the dark to etioplasts, which contain a prominent lattice-like membranous structure called the prolamellar body, with prothylakoids extending from this structure into the plastid lumen (Gunning, 1965). Upon illumination, thylakoids and the photosynthetic apparatus are synthesized and assembled within a few hours (Lopez-Juez and Pyke, 2005). This rapid differentiation of the chloroplast upon illumination requires an immediate regulation of gene transcription, protein translation, and folding. It also demands a light-sensing mechanism that regulates gene transcription of chloroplast proteins. Indeed, phytochrome-mediated signaling has been shown to be involved not only in light sensing but also in mediating transcriptional regulation by direct interaction with the phytochrome-interacting transcription factors (PIFs) and, thus, also indirect modulation of chloroplast development (Somers et al., 1991). PIF1 regulates the transcription of chlorophyll biosynthesis genes (Moon et al., 2008), whereas PIF3 is involved in chloroplast development (Monte et al., 2004; Stephenson et al., 2009).

By contrast, the majority of the chloroplasts in apical meristem-derived leaves arise primarily through fission of fully or partially differentiated chloroplasts. Consequently, it was hypothesized that there would be different regulation of the two types of chloroplast development. Indeed, mutations that affect leaves and not cotyledons have been observed; for example, the abovementioned *var2* mutant exhibits its variegated phenotype in the true leaves but not in cotyledons (Chen et al., 2000). Conversely, mutations have been identified that affect cotyledons but not true leaves. Other mutations lead either to delayed greening due to affected chloroplast gene transcription as in *sigma factor6* (Ishizaki et al., 2005) or, in *wco*, to a complete block in chloroplast biogenesis in the cotyledon due to impaired mRNA maturation (Yamamoto et al., 2000). *snowy cotyledon* (*sco*) and *cyo1* mutations were identified that disrupt chloroplast biogenesis in cotyledons but not leaves, resulting in chlorotic cotyledons and green true leaves (Albrecht et al., 2006, 2008; Shimada et al., 2007). The proteins mutated by *sco1* and *sco2*/*cyo1* are required for chloroplastic protein translation and folding, respectively, functions necessary for biogenesis.

Here, we describe the isolation and the characterization of a chloroplast biogenesis mutation, *sco3*, which unlike the aforementioned examples, is not a mutation in a chloroplast protein involved in chloroplast gene transcription, mRNA maturation, or protein translation and folding. Instead, SCO3 is localized to the peroxisomes and implicates microtubules in chloroplast differentiation.

RESULTS

sco3-1 Compromises Chloroplast Biogenesis and Structure

The *sco3-1* mutant was isolated from ethyl methanesulfonate–mutagenized *Arabidopsis thaliana* seeds as described for *sco1* (Albrecht et al., 2006). *sco3-1* cotyledons contain 20 to 40% of the chlorophyll of wild-type Columbia (Col) cotyledons and were more photoinhibited as determined by measuring maximal photosynthetic efficiency (Figure 1A, Table 1). Though cotyledons are present in the embryo, no differences in the chlorophyll content in developing *sco3-1* embryos compared with the wild type could be observed (see Supplemental Figure 1 online). In addition, precociously germinated seedlings exhibit normal green cotyledons (see Supplemental Figure 1 online), an observation also made in the characterization of the *sco2* mutant (Albrecht et al., 2008). As described for other *sco* mutants, the true leaves of *sco3-1* were green and photosynthetically similar to the wild type (Table 1). Other than the chlorotic cotyledons and a consequential slight delay in growth, there were no obvious morphological or visible developmental defects in leaves, flowers, and roots.

The effect of the *sco3-1* mutation on chloroplast and etioplast differentiation was investigated by ultrastructural analyses of etioplasts of seedlings germinated for 4 d in the dark and chloroplasts of 10-d-old seedlings germinated in the light. In wild-type dark-grown seedlings, the etioplasts contained the prolamellar body and prothylakoids. Neither were they observed in *sco3-1*; rather, the *sco3-1* plastid resembled an undifferentiated proplastid (Figure 1B). A key component of the prolamellar body is the chlorophyll precursor, protochlorophyllide (pchlide), bound to its enzyme, pchlide oxidoreductase. A 77K low-temperature fluorescence measurement at an excitation wavelength of 420 nm results in pchlide fluorescence at 630 nm. We could not detect any fluorescence for pchlide in the *sco3-1* mutant (see Supplemental Figure 2 online).

Chloroplasts in light-grown wild-type seedlings have a characteristic structure, including stacked granal thylakoids and starch granules (Figure 1C). In 14-d-old *sco3-1* seedlings the majority of the cotyledon plastids were aberrant, although in some cells there were plastids of wild-type appearance. The aberrant plastids varied in the degree of differentiation and shape (for example, see Figures 1C and 1D) with most resembling an undifferentiated plastid. However, the size and number of plastids per *sco3-1* cell were similar to those found in Col. Therefore, *sco3-1* inhibits plastid differentiation of both etioplasts and chloroplasts but not plastid enlargement or division.

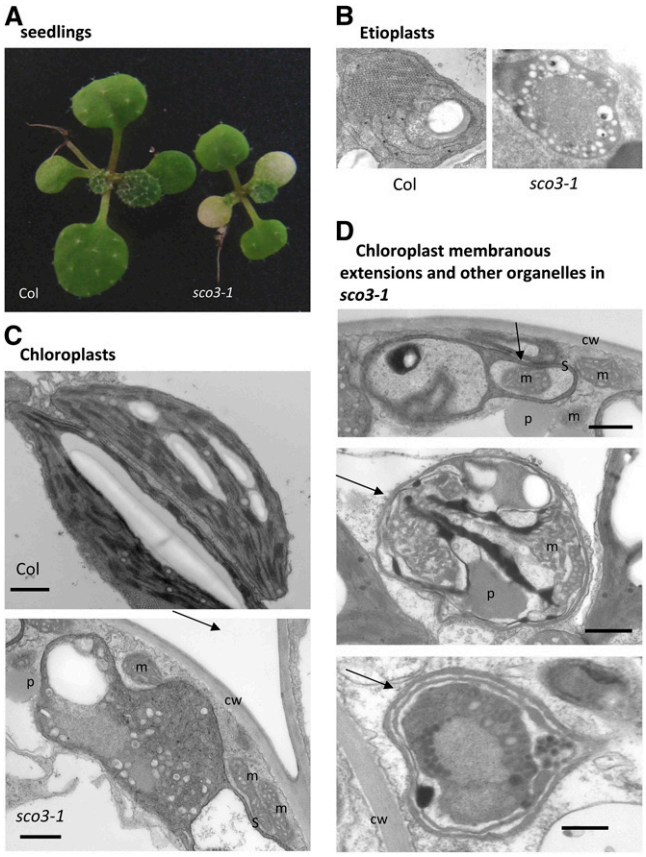

Figure 1. Phenotype of *sco3-1*.

(A) Phenotype of 14-d-old *sco3-1* seedlings compared with Col.
(B) and **(C)** TEMs of etioplasts **(B)** and chloroplasts **(C)** in cotyledons of Col and *sco3-1*.
(D) Cross sections of chloroplast membranous extensions in *sco3-1* (indicated by an arrow). Note the mitochondrial (m) and peroxisomal (p) structures within these plastids and the engulfment of a mitochondrion in the top image. S, stromule; cw, cell wall. Bars = 1 μm.

sco3-1 Does Not Alter Expression of Chloroplast-Encoded Genes and Modifies a Small Set of Nuclear-Encoded Genes

The impairment of plastid differentiation could indicate that SCO3 is required for plastid transcription; thus, a change to the expression of plastid-encoded or nuclear-encoded genes required for plastid transcription might be expected. However, there were no changes in the plastid transcriptome for any of the genes tested by RT-PCR (Figure 2A). Indeed, a global quantitative RT-PCR analysis of the entire plastid transcriptome in 4-d-old seedlings did not reveal any significant changes in expression of the plastid genome (Figure 2B; see Supplemental Figure 3 online).

As outlined, extensive bleaching of the plastid typically resulted in a repression of nuclear-encoded genes, such as the light-harvesting protein LHCB1.2. Both *sco1* and *sco2* exhibit the expected reduction of the expression of the light-harvesting protein LHCB1.2, reflecting the bleaching of the cotyledon's plastids (Albrecht et al., 2006, 2008). In another mutant, *gun1*, *LHCB1.2* expression is maintained even though chloroplast biogenesis is severely perturbed by the application of chemicals such as norflurazon or inhibitors of chloroplast translation (Koussevitzky et al., 2007). *sco3-1* shows a wild-type downregulation of gene expression in response to norflurazon treatment (see Supplemental Figure 4 online), but we did not observe any downregulation of *LHCB1.2* or *PORB* in untreated pale *sco3-1* seedlings, which is in contrast with *sco1* and *sco2* (Figures 2A and 2C). When we undertook a gene expression array using Affymetrix gene chips (ATH1), the same observation was made; that is, genes normally downregulated when chloroplast biogenesis is perturbed (e.g., *LHCB1.2*, *PORB*, and *rbcS*) were not altered in *sco3-1* (see Supplemental Data Set 1 online). The array was performed in triplicate on 4-d-old *sco3-1* and wild-type seedlings. Statistical analysis and false discovery correction were undertaken, and four genes were experimentally validated by RT-PCR (Figures 2A to 2D). Since the RT-PCR analysis showed a similarity in retrograde signaling with the *gun* mutants (Figures 2C and 2D), we performed a comparison of the identified up- or downregulated genes in *sco3-1* with array data from the *gun1-9* and *gun5* mutants using Genevestigator. The set of down- and upregulated genes of untreated *sco3-1* are similarly altered in expression in *gun1-9* and *gun5* treated with norflurazon (see Supplemental Figures 5A and 5B online), indicating that the bleached *sco3-1* mutant is responding at the gene expression level similar to treated *gun* mutants. This indicates either that *sco3-1* is disrupting the signaling from the chloroplasts to the nucleus similar to what has been observed in the *gun* mutants or that there is a sufficient number of functional chloroplasts able to elicit wild-type levels of nuclear gene expression (see Discussion).

Using MapMan to catalog the identified genes, no consistent changes in genes associated with photosynthesis or primary or secondary metabolism could be seen (Figure 2E; see Supplemental Figure 6 online). Analysis of the predicted localization of differentially regulated genes in *sco3-1* showed a surprisingly low number of genes encoding chloroplast-localized proteins being downregulated in the mutant (15 genes), with three of them involved in photosynthesis and five in Leu or Trp biosynthesis (Figure 2E; see Supplemental Figures 5C and 6 online). On the other hand, >40% of the downregulated genes encode proteins localized to the membrane/endomembrane system involved in transport or carbohydrate or lipid metabolism (see Supplemental Data Set 1 online). Only five transcription factors are downregulated in *sco3-1*, one of them being GLK1, which has been shown to be involved in the transcription of photosynthesis genes (Waters et al., 2009). However, just four of the 154 genes predicted to be GLK1 regulated are affected in *sco3-1*. Eighteen of the 80 genes upregulated in *sco3-1* encode chloroplast-targeted proteins, although most of them are of unknown function (Figure 2E; see Supplemental Figure 5D online). Interestingly, 68 of 80 genes (85%) upregulated in *sco3-1* have low or undetectable levels of expression in all three Col biological replicates (Figure 2E; see Supplemental Figure 7 online). Similarly, 92 of 123 (75%) of those downregulated compared with Col are undetectable in all three *sco3-1* biological replicates.

The development of the seedling and formation of the chloroplasts is stimulated by light acting via phytochrome-mediated

Table 1. Comparison of *sco3*-1 to Col

	Chlorophyll Content (mg Chlorophyll/mg Fresh Weight)		Photosynthetic Efficiency (F_v/F_m)		Growth under High CO_2	F2 Outcross Segregation
Line	Cotyledon	Leaves	Cotyledon	Leaves	Plants	Pale:green
Col	0.78 ± 0.01	0.65 ± 0.01	0.65 ± 0.04	0.66 ± 0.02	Green	
sco3-1	0.23 ± 0.09	0.69 ± 0.08	0.59 ± 0.03	0.61 ± 0.04	Small, pale	154:726
sco3-1 + *SCO3*	0.64 ± 0.25	0.67 ± 0.11	n.a.	n.a.	Green	57:266
sco3-1 + M*SCO3-1*	0.33 ± 0.12	n.a.	n.a.	n.a.	n.a.	n.a.

Chlorophyll content, photosynthetic efficiency, growth under high CO_2, and F2 outcross to wild-type segregation analysis for Col, *sco3-1*, and *sco3-1* complemented with GFP:*SCO3* and GFP:M*SCO3-1*, respectively. The mean and SD are shown for at least 3 × 30 mg samples for chlorophyll and 3 × 20 seedlings for F_v/F_m analysis. n.a., not analyzed.

pathways. Indeed, PhyB and its interacting transcription factors, such as PIF3, are crucial in the regulation of genes encoding chloroplast proteins such as the LHCBs (Monte et al., 2004; Castillon et al., 2007). To determine if the impairment of chloroplast biogenesis in *sco3-1* is related to phytochrome signaling, we generated *sco3-1 phyB* and *sco3-1 phyA* double mutants. The transcripts examined did not change in *sco3-1 phyA*, and two of the four genes were unchanged in the *sco3-1 phyB* double mutants (Figures 2C and 2D). Thus, *sco3-1* does not disrupt the expression of plastid- or nuclear-encoded genes required for plastid gene transcription and translation. Furthermore, *sco3-1* does not result in the expected repression of *LHCB1.2* gene expression despite extensive bleaching of the plastid.

SCO3 Encodes a Protein of Unknown Function Unique to Vascular Plants

The *sco3-1* mutation was identified by map-based cloning to be a point mutation in the gene At3g19570, 22 bp after the start of translation (Figure 3A; see Supplemental Figure 8 online). The point mutation leads to an amino acid change from Gly to Glu (G8E). Insertional mutant populations were screened for lesions in At3g19570, and three more *sco3* alleles (SALK_130239, *sco3-4*; SALK_065781, *sco3-2*; and SALK_09815, *sco3-3*) were identified. However, all three knockouts of *SCO3* cause an early embryo-lethal phenotype (Figure 3B). Crosses of homozygous *sco3-1* with heterozygous SALK_120239 resulted in aborted embryos in the F1 progeny, thereby confirming the allelism of *sco3-1* and *sco3-4*. Eight independent transgenic *sco3-1* lines containing a wild-type copy of At3g19570 (*SCO3*) developed green cotyledons, confirming *sco3-1* as a lesion in At3g19570 (Figure 3C, Table 1). Furthermore, chlorophyll content in these complemented mutant lines almost reached the wild-type level (Table 1). This is in contrast with the *sco3-1* seedlings transformed with the cDNA of *SCO3* containing the *sco3-1* (*Msco3-1*) mutation, which was not able to complement the pale cotyledon phenotype (Figure 4D, Table 1). Segregation analysis of green seedlings in the T2 generation of *sco3-1* mutant seedlings containing the *SCO3* wild-type transgene further confirmed that the mutation in At3g19570 is responsible for the pale cotyledon phenotype.

The *SCO3* gene, At3g19570, encodes a protein of unknown function consisting of 644 amino acids. Computational analyses predicted a myristoylation site, a SON-like domain, and a large, conserved domain of unknown function (DUF566, MIPS *Arabidopsis thaliana* database; Figure 3E). SON proteins are known from humans to be involved in the negative regulation of hepatitis B (Oswald et al., 2001). The *sco3-1* mutation, G8E, is located in a predicted myristoylation site with Gly being the amino acid required for the lipid modification (Sorek et al., 2009). Eight other proteins in *Arabidopsis* were identified as containing the DUF566 domain, as were proteins from other plant species such as rice (*Oryza sativa*), grape (*Vitis vinifera*), and banana (*Musa* spp), as well as the moss *Physcomitrella patens* (see Supplemental Table 1 online). Phylogenetic analysis of the proteins from the different plant species showed a clear separate clustering of the proteins from *Physcomitrella*, indicating that these proteins differ from those in vascular plants (see Supplemental Figure 9 online). An alignment of the *Arabidopsis* proteins showed that toward the C terminus, most of them exhibited a highly conserved QWRF amino acid sequence that is also present in the proteins of the other plant species (see Supplemental Figure 10 online), but this domain is not found in animal SON proteins. Thus, we named these proteins as QWRF proteins and SCO3 as QWRF1 (see Supplemental Table 1 online). Half of these proteins are predicted to be localized to chloroplasts. To date, one member of the QWRF family, QWRF5, has been studied, and it was shown to be a microtubule-associated protein that when knocked out by the *endosperm defective1* mutation is embryo lethal (Pignocchi et al., 2009).

SCO3 mRNA is detectable at low levels after 50 cycles of PCR in young developing tissues, such as seedlings, roots, flowers, and buds as well as young siliques and to a lesser extent in mature green tissues (Figure 3F). In the database, *SCO3* has a predicted second splice variant for the mRNA, which would result in altered splicing of the penultimate exon and the following intron. However, no mRNA could be detected using primers specific for this splice variant (Figure 3F). Furthermore, this predicted second splice variant of *SCO3* is not represented in published ESTs (The Arabidopsis Information Resource and SALK). Thus, only one splice variant of *SCO3* appears to be present in *Arabidopsis. SCO3* mRNA is induced by the chloroplast-bleaching herbicide norflurazon in both *sco3-1* and wild-type seedlings (Figure 3D).

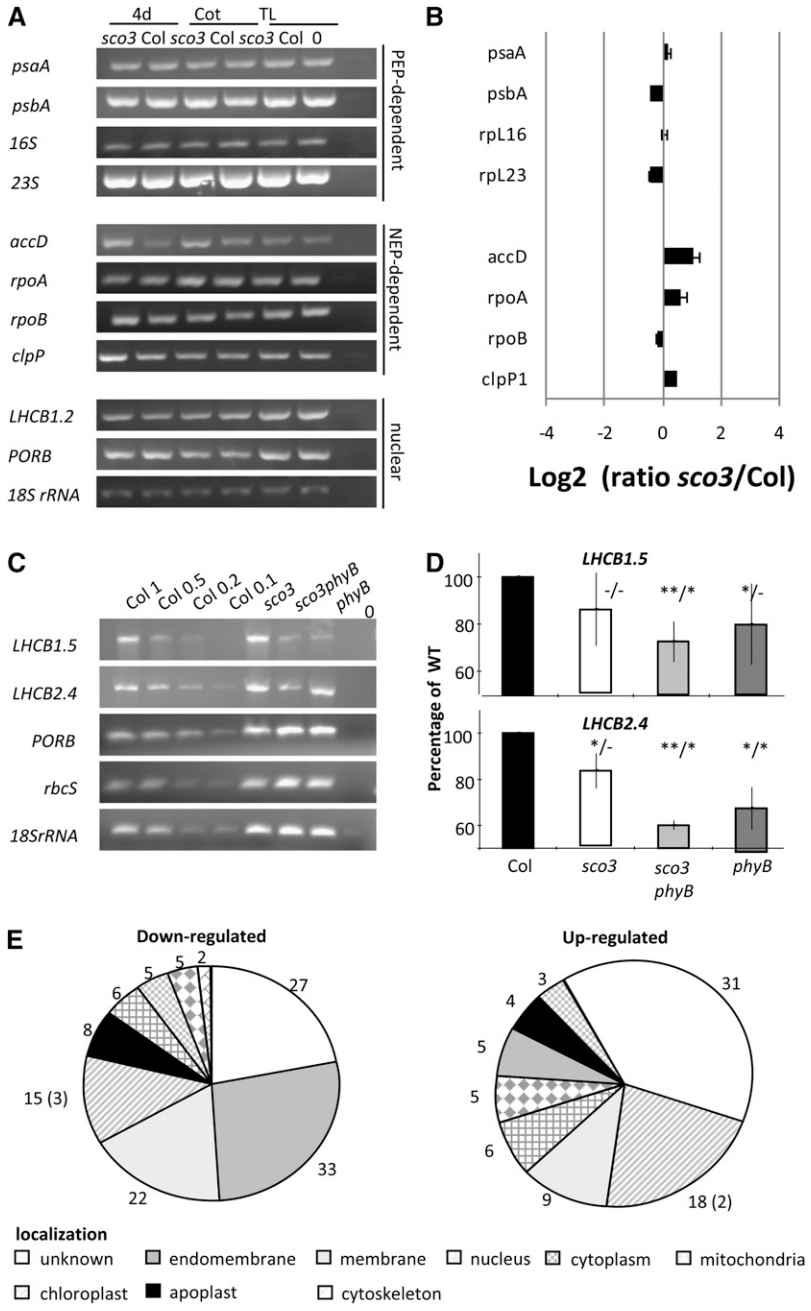

Figure 2. Transcript Analyses of Plastid-Encoded and Nuclear-Encoded Genes.

(A) RT-PCR analysis of transcripts of plastid genes dependent on nuclear-encoded (NEP) or plastid-encoded (PEP) polymerase as well as of nuclear-encoded genes regulated by retrograde signaling in 4-d-old seedlings (4d) and from cotyledons (cot) and true leaves (TL) of 14-d-old seedlings of *sco3-1* and Col. "0" is the negative control with no cDNA added to the reaction.

(B) Quantitative RT-PCR analysis of the plastid-encoded genes of 4-d-old seedlings of *sco3-1* compared with Col. Analysis was performed with three independent replicates.

(C) RT-PCR analysis of nuclear-encoded genes regulated by retrograde signaling in 4-d-old seedlings of *sco3*, *sco3 phyB*, and *phyB* compared with Col.

(D) Comparison of transcript levels of *LHCB1.5* and *LHCB2.3* compared with Col (WT). *P < 0.05; **P < 0.005; compared with wild type/compared with *sco3-1.* Error bars indicate the SD. Analysis was performed in triplicates.

(E) Predicted subcellular localization of down- and upregulated genes in *sco3-1* compared with Col from the microarray analysis. Numbers in brackets indicate the number of photosynthesis-related genes.

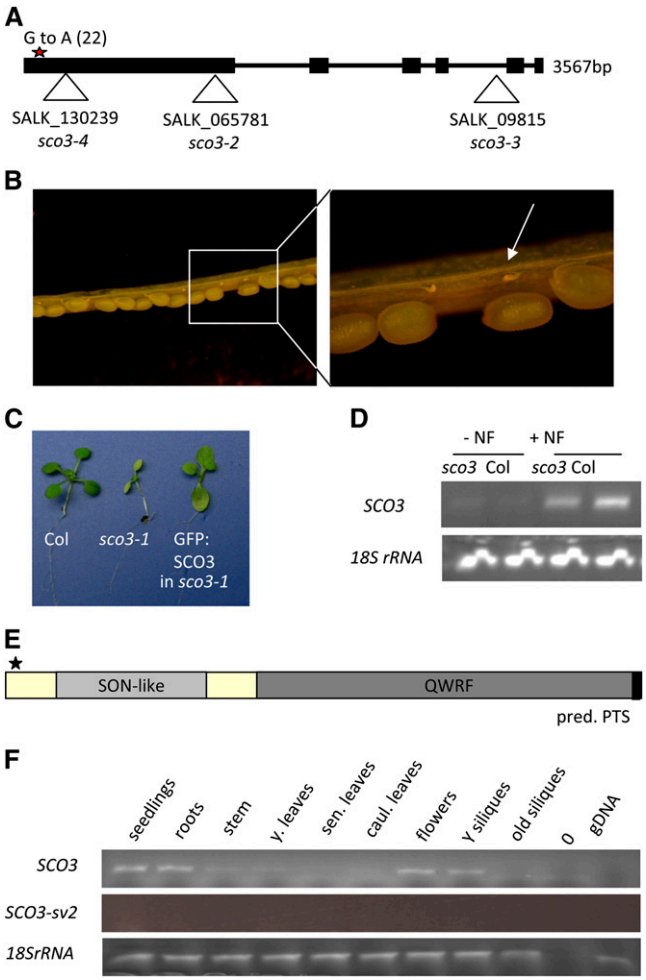

Figure 3. Characterization of the *SCO3* Gene.

(A) Structure of the *SCO3* gene. The mutation in *sco3-1* is marked with a star. The positions of the T-DNA insertion lines from SALK are indicated.
(B) Embryo-lethal phenotype of the *sco3* T-DNA insertion mutant (shown for SALK_120239). Embryo development stopped at a very early developmental stage (see arrow for an early aborted embryo).
(C) Complementation analysis of the *sco3* mutant with the *SCO3* cDNA using the GFP:SCO3 construct.
(D) RT-PCR analysis of *SCO3* transcripts in the *sco3-1* mutant and in Col in 4-d-old seedlings grown on MS media without (−NF) or with norflurazon (+NF) using 18S rRNA as loading control.
(E) Domain structure of the SCO3 protein. The star marks the position of the mutation in *sco3-1*. pred. PTS, predicted peroxisome targeting sequence.
(F) Transcript abundance of *SCO3* and *SCO3-sv2* in different plant organs and developmental stages.
Note that 25 cycles were used for the RT-PCR for the *18SrRNA* control and 50 cycles for *SCO3* in **(D)** and **(F)**. y, young; sen., senecescent; 0, negative control without DNA added into the reaction; gDNA, genomic DNA control for specificity for cDNA.

Localization of SCO3 to Peroxisomes Is Necessary for Its Function

The localization of SCO3 had not been experimentally determined, and the targeting prediction programs at SUBA (Heazlewood et al., 2007) gave inconclusive or conflicting results. Therefore, to determine the subcellular location of SCO3, a series of green fluorescent protein (GFP) fusion constructs were generated and transiently expressed in biolistically transformed cell culture. Interestingly, GFP:SCO3 showed a small punctuate fluorescence pattern that predominantly colocalized with peroxisomes (Figure 4A) with just a small subset of the GFP:SCO3 fluorescence not being associated with the peroxisomal targeted red fluorescent protein (RFP):SRL (containing the peroxisome targeting sequence 1 motif). Indeed, SCO3 contains the C-terminal PTS1 peroxisomal targeting domain, SRL (Reumann, 2004). Whereas GFP:SCO3 was unequivocally localized to the peroxisomes, it was not distributed throughout the organelle; rather, the GFP fluorescence appeared at discrete smaller spots, potentially associated with the surface of peroxisomes. The peripheral localization of GFP:SCO3 could also be observed in a heterologous system using transformed onion cells (Figure 4C). Here, the localization at the surface of the peroxisomes was more obvious when observed together with the movement of the peroxisomes. The GFP fluorescence of SCO3 moved as the organelle turned around its axis (see Supplemental Movie 1online). Furthermore, some of the GFP-labeled SCO3 proteins appeared to transiently dissociate from the peroxisome but rapidly return to the peroxisome surface. However, whether this dissociation reflects in vivo movement or a possible artifact from using two channels of the confocal microscope is unclear. Peroxisomes, like chloroplasts and mitochondria, have membranous extensions (Sinclair et al., 2009). It would be interesting to investigate if SCO3 might be involved in the formation of these membranous extensions, called peroxules. SCO3 is likely to be the only member of the QWRF family with a peroxisomal location as none of the others contain the peroxisomal targeting sequence. A mutated version of SCO3 lacking the peroxisome targeting sequence at the C terminus, GFP:SCO3ΔSRL, was not able to complement the *sco3-1* mutant phenotype (Figure 4D). The mutation in *sco3-1* affects a putative myristoylation site, and the posttranslational addition of a lipid, myristate, targets proteins to membranes. Therefore, we tested targeting with mutated SCO3 (Figures 4B and 5C). The results showed that the SCO3 mutation does not affect localization of the protein to the peroxisome (Figure 4D).

Some prediction programs indicated that SCO3 could be chloroplast targeted, although the scores were relatively low. However, in vitro import assays performed with radioactive-labeled SCO3 protein did not show any import of SCO3 into isolated *Arabidopsis* chloroplasts (Figure 5A). As recommended by Millar et al. (2009), multiple lines of evidence should be obtained for targeting. As already stated, the GFP:SCO3 fusion did not colocalize with chloroplasts but rather with the peroxisome (Figures 4 and 5B). To test if the putative chloroplast transit peptide was functional, a SCO3:GFP fusion protein was created but did not result in any detectable GFP fluorescence (it would not go to the peroxisome as the C-terminal GFP would mask the

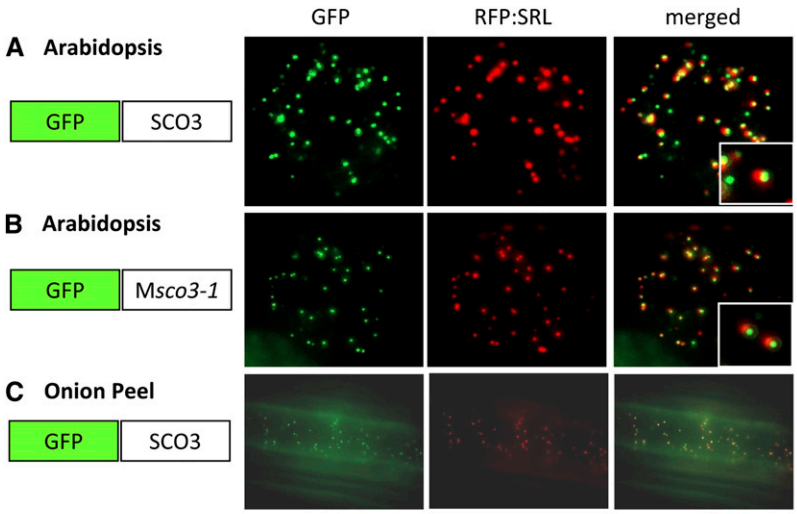

D Transformation of sco3-1 with SCO3 constructs

Construct	WT	PTS	Complement
GFP:SCO3	Y	Y	+
GFP:SCO3ΔSRL	Y	N	-
GFP:Msco3-1	N	Y	-

Figure 4. Localization of the SCO3 Protein.

(A) and **(B)** Localization studies were performed using N-terminal GFP fusions with the complete SCO3 **(A)** or mutated SCO3 (*Msco3-1*). RFP:SRL is used to visualize peroxisomes using peroxisome-targeted RFP **(B)**. Insets in **(A)** and **(B)** magnify the GFP signal on peroxisomes.
(C) Localization of GFP:SCO3 to the periphery of peroxisomes in a heterologous system, onion (see Supplemental Movie 1 online).
(D) Complementation analyses, as determined by chlorophyll content in cotyledons using different wild-type (WT) SCO3 cDNA constructs with an N-terminal GFP (green box) and with or without the PTS (orange box) and N-terminal GFP fused to SCO3 cDNA containing the *sco3-1* mutation (star).

PTS). Constructs containing just the first 100 amino acids of wild-type or mutated SCO3, fused N-terminally to GFP, resulted in a diffuse fluorescence signal that did not indicate any discrete location consistent with a plastid localization (Figures 5B and 5C).

To test further if transgenically targeting SCO3 to the chloroplast could complement the *sco3-1* phenotype, we transformed *sco3-1* with SCO3:GFP and a construct comprising the chloroplast transit peptide of the small subunit of ribulose-1,5-bisphosphate carboxylase/oxygenase (Rubisco) fused to SCO3, SSUcTP:SCO3:GFP. Neither construct resulted in complementation of the mutant phenotype in *sco3-1* (Figure 5C). Thus, only the wild-type version of SCO3, with an accessible peroxisome targeting signal, is able to complement the mutant phenotype.

sco3-1 Does Not Alter Germination or Peroxisomal Fatty Acid β-Oxidation

Peroxisome functions include the mobilization of storage compounds during germination, fatty acid β-oxidation, and photorespiration, the latter involving chloroplasts and mitochondria (Foyer et al., 2009). Mutants affected in the mobilization of storage compounds are not able to germinate without exogenous application of sucrose. Since the *sco3-1* mutant is able to germinate without sucrose in soil or media, the mutant is not affected in this process. One method to analyze fatty acid β-oxidation is to apply indole-3-butyric acid (IBA), which is converted through β-oxidation to auxin, which then affects root growth and hypocotyl elongation in etiolated seedlings. However, etiolated IBA-treated *sco3-1* seedlings were indistinguishable from the IBA-treated wild type (Figure 6A), indicating no impairment to fatty acid β-oxidation in *sco3-1*.

The *sco3-1* Mutant Does Not Affect Photorespiration but Does Exhibit Low-CO_2 Sensitive Photoinhibition

Alterations in photorespiratory function can be analyzed by examining the growth and physiology of plants at high and low CO_2 (Figures 6B and 6C). Typical photorespiration mutants are not able to grow normally under air CO_2 levels but can be rescued by growth under high CO_2. *sco3-1* grows in air, so it is not a typical photorespiratory mutant (Schumann et al., 2007; Foyer et al., 2009).

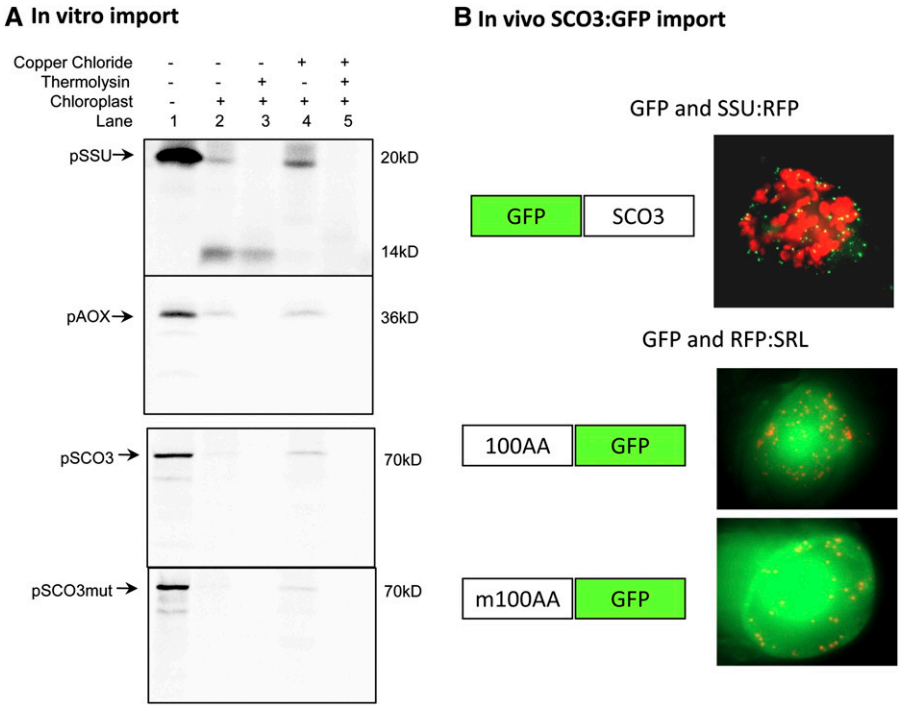

C Transformation of *sco3-1* with chloroplast targeting of SCO3

Construct	Chlc TP	PTS acc	Complement
GFP:SCO3	N	Y	+
SCO3:GFP	N	N	-
SSUcTP:SCO3:GFP	Y	N	-

Figure 5. The SCO3 Protein Is Not Localized to the Chloroplast.

(A) In vitro import analysis of radioactively labeled SCO3 and mutated SCO3 (SCO3mut) into isolated *Arabidopsis* chloroplasts. pSSU, the precursor of the small subunit of Rubisco was used as a positive control and the mitochondrial-targeted pAOX (alternative oxidase) as a negative control for chloroplast import of proteins. Copper chloride is inhibiting chloroplast protein import, whereas thermolysin degrades all not-imported proteins in the solution.

(B) Localization studies were performed using the first 100 amino acids of SCO3 or mutated SCO3 (m100AA, with the *sco3-1* mutation) fused to C-terminal GFP. SSU:RFP was coexpressed to visualize chloroplasts.

(C) Complementation analyses showing the complementing GFP:SCO3 and using additional SCO3 constructs with a C-terminal GFP (green box, in which the PTS is not accessible) to unmask the putative chloroplast transit peptide and with the fusion of the chloroplast targeting sequence (Chl cTP) of rcbS (SSUcTP; dark-green box), respectively.

sco3-1 seedlings showed a reduced maximal PSII efficiency, F_v/F_m, under high CO_2 growth conditions. This was apparent not only in cotyledons of 7-d-old seedlings (F_v/F_m of 0.42 $\pm$ 0.14 for *sco3-1*) but also in the true leaves of 14-d-old plants (F_v/F_m of 0.49 $\pm$ 0.08 for *sco3-1*; Figure 6B). After transfer to zero CO_2, both 7- and 14-d-old seedlings showed a dramatic reduction of the F_v/F_m values (from 0.49 to 0.15 $\pm$ 0.1 for both) in the mutant seedlings, whereas wild-type seedlings exhibited only a slight reduction in PSII efficiency. On the other hand, if mutant seedlings were transferred to ambient CO_2 concentrations, a recovery of PSII efficiency was observed. When the same experiment was performed with seedlings grown under ambient CO_2, transfer to zero CO_2 for 24 h caused only a slight reduction in F_v/F_m. Consistent with this, there is a clear growth phenotype in mature *sco3-1* plants grown under high CO_2, whereas *sco3-1* plants grown in air are indistinguishable from the wild type at maturity (Figure 6C). Rosette leaves of *sco3-1* plants grown in high CO_2 conditions are pale green and rounded, and the whole rosette is smaller compared with the wild type (Figure 6C). The unifying explanation for what appears to be both a low CO_2 and high CO_2 phenotype in *sco3-1* is not obvious from our experiments but may be related to the peroxisome metabolism at different stages

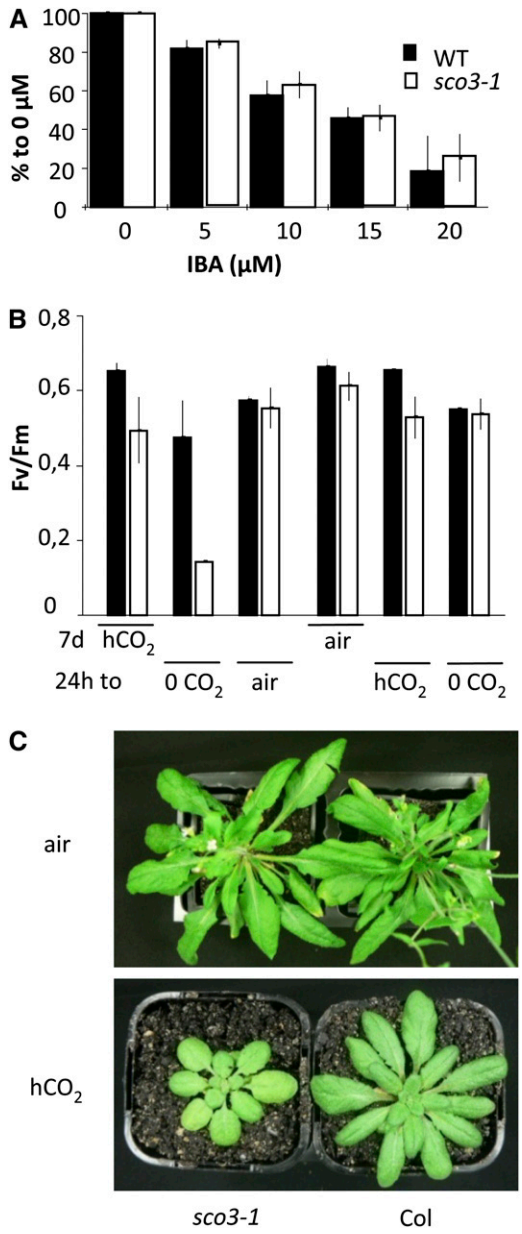

Figure 6. Analysis of Peroxisomal Function.

(A) Analysis of β-oxidation processes using IBA, which is β-oxidized in peroxisomes to auxin. Hypocotyl length of etiolated seedlings at different concentrations of IBA was measured and is expressed as the percentage of the hypocotyl length of seedlings of the same genotype grown without IBA application. The error bars define the SD of three independent replicates. WT, wild type.

(B) Effects on photorespiration and photoinhibition. Seedlings of Col (black box) and *sco3-1* (white box) were grown for 7 d under high CO_2 (hCO_2, 0.6%) or at ambient CO_2 concentration (air) and, after measuring the activity of PSII (F_v/F_m), were transferred for 24 h to altered CO_2 concentrations (0 CO_2, air, or hCO_2). F_v/F_m was measured again.

(C) Phenotype of plants grown for 5 weeks either at ambient CO_2 (air) or under high CO_2 (hCO_2).

of development. Taken together, the *sco3-1* mutation affects not only chloroplast biogenesis in seedlings but also chloroplast function in cotyledons and mature leaves under altered CO_2 conditions.

Cytoskeleton Inhibitors Phenocopy *sco3-1* Plastid Morphology

Since the aforementioned peroxisomal functions in *sco3-1* are similar to those in wild-type plants, other aspects of cellular function were examined. Confocal microscopy revealed a reduction in chlorophyll fluorescence in most of the plastids of *sco3-1* cotyledons (Figure 7A). GFP-labeled plastids in *sco3-1* that lacked or had reduced chlorophyll fluorescence were comparable in size and could import GFP (cf. image to top right inset in Figure 7A), supporting the hypothesis that the plastids that have failed to differentiate could still import GFP. Furthermore, immunoblot analysis on total protein extracted from 4-d-old seedlings did not show any unprocessed LHCB2 protein (see Supplemental Figure 11 online).

Interestingly, we also observed bilobed plastids in *sco3-1* (Figure 7A, bottom right inset). Bilobed plastids could be considered as being arrested or affected in chloroplast division. However, chloroplast division mutants typically have larger and fewer plastids, without a bilobed structure (Glynn et al., 2007). Analyzing the confocal micrographs, only 14% of the 163 cells analyzed in *sco3-1* resemble normal cells containing a wild-type number of functional chloroplasts, whereas 24% of the cells contained a mixed population of functional and abnormal plastids, 36% had solely abnormal plastids, and in 25% of the cells, we were not able to detect any functional chloroplasts at all. The observed number of functional chloroplasts can account for the considerable (although compared with the wild type, dramatically reduced) F_v/F_m values measured in *sco3-1*. Even a leaf under stress, such as drought, and that will not recover when rewatered, can have an F_v/F_m of ~0.3 (Woo et al., 2008).

We tested cytoskeleton inhibitors to determine if they could result in bilobed plastids (Kwok and Hanson, 2003). Inhibition of the cytoskeleton with either amiprophosmethyl (APM) for microtubules or cytochalasin D (CD) for microfilaments resulted in more of the smaller plastids and bilobed plastids in *sco3-1* (Figure 7B). More importantly, treatment of Col with APM resulted in very similar plastid morphology and chlorophyll fluorescence to that observed in untreated *sco3-1*. Furthermore, treating seedlings with APM under a range of conditions resulted in a reduction of chlorophyll accumulation to 60 to 70% of wild-type levels (Figure 8, Table 2). The effect of CD treatment (leading to 80% of chlorophyll accumulation compared with untreated wild type) was more subtle (Table 2). Treatment of cells containing GFP:SCO3 with APM resulted in a complete loss of the GFP:SCO3 signal and affected peroxisome morphology (Figure 8).

Not only do *sco3-1* plastids resemble enlarged proplastids, some of them also have membranous extensions that in some ways, but not others, resemble retracted or looped stromules encompassing cytoplasm (Figure 1D). Stromules have been implicated in plastid–cytoskeleton interactions (Kwok and Hanson, 2003). A further indication for a role related to microtubules can be implied by the stringent analysis of coexpressed genes

under different plant developmental stages and plant organs. Using databases, such as AttedII (http://atted.jp/), 8% of the genes coexpressed with *SCO3* are associated with the cytoskeleton, and one of them, *TUBULIN7*, is also downregulated in *sco3-1.* For reference, AttedII also shows that *SCO2* coexpressed genes were largely related to chloroplast transcription and translation, but none were cytoskeleton related. Furthermore, some cytoskeleton-associated genes are downregulated in *sco3-1*, but none are differentially regulated in the *gun* mutants.

It has already been demonstrated that the actin cytoskeleton is involved in several aspects of chloroplast biology, such as the relocation of the chloroplasts in response to shade/high light (Kadota et al., 2009), inheritance of organelles during plant cell division (Sheahan et al., 2004), and chloroplast protein import (Jouhet and Gray, 2009). To determine if there were changes to the structure of the cytoskeleton in *sco3-1*, we undertook transient transformation of Col and *sco3-1* cotyledons with talin:GFP for visualizing the actin filaments (Figure 7C) (Hardham et al., 2008). In transformed Col cells, a complex network that included fine structure was repeatedly observed. However, whereas *sco3-1* had a similar coarse structure, we never observed the fine actin filaments that were apparent in Col (Figure 7C). Thus, *sco3-1* appears to alter the cytoskeleton, and disrupting the cytoskeleton impairs GFP:SCO3 targeting to the peroxisome.

DISCUSSION

A Peroxisomal Protein Is Required for Plastid Development

SCO3 is required for chloroplast and etioplast biogenesis in seedlings. In its absence, most plastids fail to differentiate, many lack chlorophyll and thylakoids, and a lot of the plastids are bilobed and have permanent membranous extensions that encapsulate other cytosolic components. Some do differentiate and are phenotypically wild-type: This could reflect the observation that *sco3-1* is not a knockout mutation. Although on the transcriptional level untreated *sco3-1* resembles a norflurazon-treated *gun* mutant, it should be noted that norflurazon treatment does suppress *LHCB* mRNA. The presence of LHCB mRNA in untreated *sco3-1*, though, could be explained by the presence of sufficient viable chloroplasts in *sco3-1* cells to elicit nuclear gene expression of LHCB. Alternatively, *sco3-1* may partially alter GUN-like signaling and, given that *sco3-1* differs from *sco2* and *sco1*, which have similar levels of chlorophyll, both alternatives are valid hypotheses at this stage. Furthermore, chloroplast division appears to occur normally in *sco3-1* since it does not resemble chloroplast division mutants, which exhibit enlarged and few chloroplasts per cell (Marrison et al., 1999; Glynn et al., 2007).

None of the factors that typically perturb chloroplast biogenesis can explain the *sco3-1* mutant phenotype. First, disruption to phytochrome-mediated signaling is not a primary cause, as both dark-grown and light-grown plastids were altered and double mutants did not reveal a clear role for SCO3 in phytochrome-mediated signaling, although there are secondary interactions. Second, transcriptome analyses showed that changes in the mRNA abundance of chloroplast-encoded or nuclear-encoded genes are not the primary cause of the *sco3-1* phenotype. Third, *sco3-1* plastids can import GFP and LHCB, indicating a functional import apparatus, although we cannot rule out that protein import is slowed down or inhibited for a specific protein. Fourth, the plastids that do differentiate are photosynthetically competent, indicating no complete loss of any component required for assembly and function of the photosynthetic apparatus. Furthermore, all aspects of photosynthesis are unaffected in mature leaves, except for photoinhibition under extreme CO_2 concentrations.

SCO3 Reveals a Role for Peroxisomes and Microtubules in Chloroplast Development

Chloroplast biogenesis is part of photomorphogenesis, which also includes morphological and physiological changes to the seedling (Chory, 1991). To date, there have been no reports of a peroxisomal protein being required for chloroplast biogenesis and only one report of a peroxisomal protein, PEX2, being implicated in photomorphogenesis (Hu et al., 2002). In that case, *de-etiolated 1*, which exhibits morphological aspects of photomorphogenesis in the dark, can be complemented by a dominant second site mutation in PEX2 (Hu et al., 2002). The question is how can a mutation in the peroxisomal-targeted SCO3 protein impair chloroplast biogenesis? The unexpected peroxisomal location of SCO3 led us to investigate peroxisomal metabolism. However, there were no changes to germination, fatty acid β-oxidation, or photorespiration. However, there were changes in photoinhibition in response to altered CO_2 and that may suggest a role for SCO3 in peroxisomal photorespiration and thus warrants further investigation. However, this change could not be the cause of impaired chloroplast biogenesis.

Given that there are no changes in chloroplast transcription or peroxisome metabolism that could account for the disruption to chloroplast biogenesis, other alternatives should be considered. This could include disruptions to protein targeting, import, and assembly; organelle division; or interactions mediated by other cellular compartments, such as the cytoskeleton. Chloroplast-targeted GFP was imported into *sco3-1* plastids, suggesting a functional import apparatus, although more subtle changes cannot be discounted at this stage. There is, however, evidence that changes to the cytoskeleton can explain many attributes of the *sco3-1* phenotype.

The chloroplast membrane extensions observed in *sco3-1* might be hypothesized to be an indirect result of the block in plastid development (Gunning, 2005; Natesan et al., 2005); however, they have not been described for any other similar chloroplast biogenesis mutants. Formation of stromule-like structures has been described for alpine plants such as *Oxyria digyna* or in other species depending on light intensity or temperature (Buchner et al., 2007; Holzinger et al., 2007; Lütz and Engel, 2007). Furthermore, in *Arabidopsis*, engulfment of other organelles such as mitochondria has also been observed in the *vtc2* mutant exhibiting low concentrations of vitamin C (Olmos et al., 2006). Alternatively, the presence of persistent chloroplast membrane extensions could reflect a disruption to organelle interactions with the cytoskeleton. Indeed, it has been shown

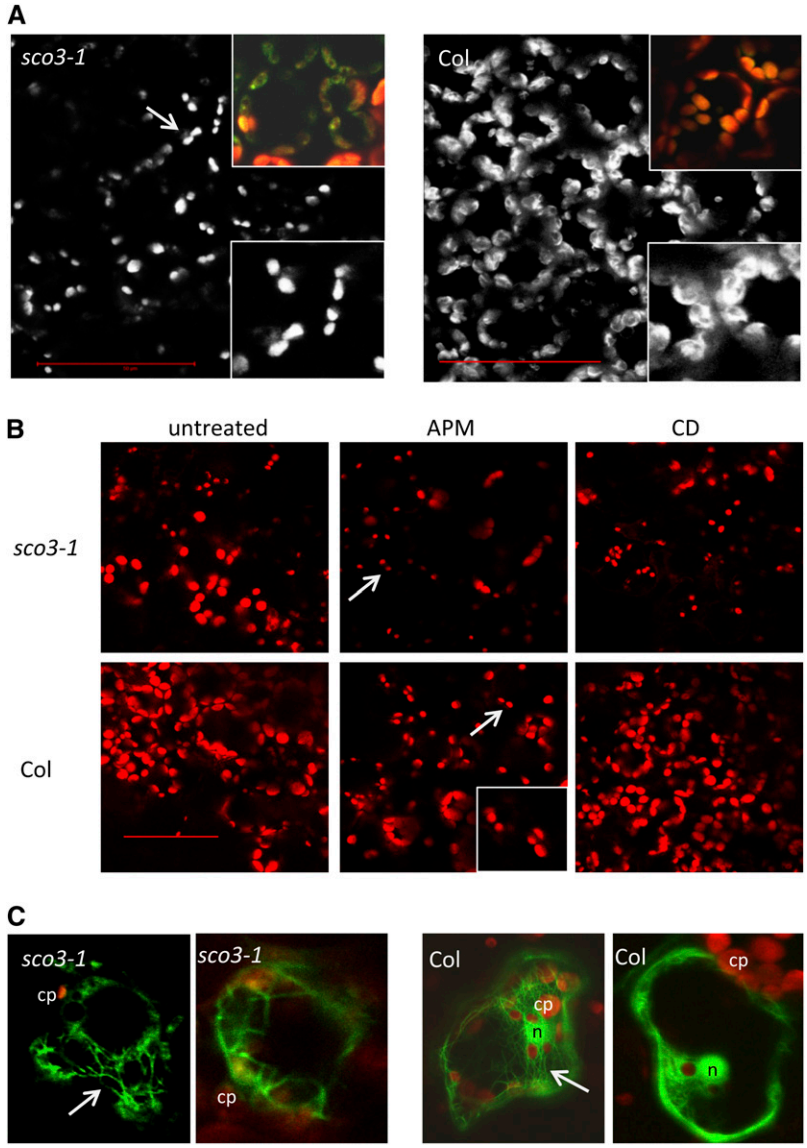

Figure 7. Chloroplasts and the Cytoskeleton.

(A) Analysis of chloroplast development in cotyledons under the confocal microscope. Chloroplasts are visible due to the autofluorescence of chlorophyll. In *sco3-1*, many plastids resemble bilobed chloroplasts (indicated by an arrow), which is magnified in the bottom right insets. In Col, no such structure could be observed. Top right insets show cpTP:GFP to visualize plastids without chlorophyll autofluorescence (chlorophyll autofluoroescence is visualized by the red color). Bars = 50 μm.

(B) Effect of cytoskeleton inhibitors APM (microtubule inhibitor) and CD (actin inhibitor) on chloroplast biogenesis in seedlings grown for 3 d on MS media before being transferred to inhibitor-containing media for an additional 2 d. Chloroplasts were visualized under the same magnification using chlorophyll autofluorescence with confocal laser scanning microscopy. The inset in APM-treated Col seedlings shows an example of bilobed chloroplasts in Col. Arrows indicate the bilobed plastids.

(C) Visualization of the actin cytoskeleton using Talin:GFP in transient transformation of seedlings of *sco3-1* and Col. Two examples for each line are shown. Arrows indicate the fine structure missing in *sco3-1* but present in Col, respectively. cp, chloroplast; n, nucleus.

that stromule morphology and movement does depend on microfilaments and microtubules and that myosin IX is involved in the movement of the stromules (Kwok and Hanson, 2003; Natesan et al., 2005, 2009). On the other hand, the double-membrane structures containing different organelles observed in *sco3-1* (Figure 1D, bottom panels) might also be interpreted as autophagosomes that target affected organelles to the vacuole. Autophagosomes have been shown to occur in plants during senescence as well as in seedlings under abiotic stress (Ketelaar et al., 2004; Ishida et al., 2008; Slavikova et al., 2008).

Most significantly, many of the phenotypes of *sco3-1*, namely, less chlorophyll, variable degrees of plastid biogenesis, and

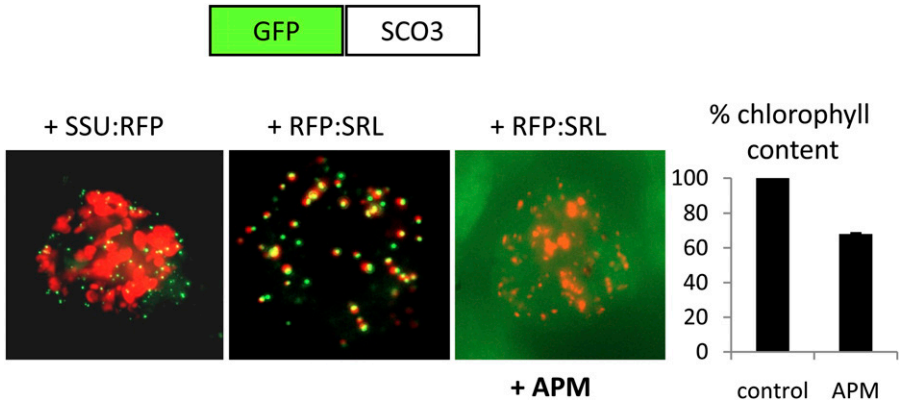

Figure 8. Model for the *sco3-1* Phenotype.

Despite the pale cotyledon phenotype in *sco3-1*, the SCO3 protein (shown as a GFP fusion) is not localized to the chloroplast (cf. the GFP signal to the red signal of chloroplast-localized SSU:RFP in the left image) but to the periphery of peroxisomes (cf. GFP to the peroxisomal RFP:SRL in the middle image). This peripheral localization on peroxisomes of SCO3 is disrupted when the microtubule cytoskeleton assembly is inhibited by APM (+APM, right image). Application of this inhibitor also results in reduced chlorophyll content as well as impaired chloroplast biogenesis and bilobed chloroplasts in the wild type that resemble those in untreated *sco3-1* (refer to Figure 7B). This demonstrates a requirement for the cytoskeleton and SCO3 in chloroplast and peroxisome biogenesis and morphology.

bilobed plastids, can be phenocopied by applying a microtubule inhibitor to wild-type Col. Furthermore, the *sco3-1* mutation perturbs the fine structure of the actin filaments and alters expression of microtubule-associated genes. So apparently, *sco3-1* results in changes to the cytoskeleton that impairs chloroplast biogenesis. Indeed, we could observe a link between the microtubule cytoskeleton and the peroxisomal localization of SCO3, which is lost when the assembly of microtubulin is inhibited. How can this observation explain the pale cotyledon phenotype in *sco3*-1? One hypothesis is that, although the import of proteins into the chloroplasts of *sco3-1* is functional (Figure 7), there might be a delay or impairment of the delivery of one or more specific plastid proteins to the organelle due to perturbation to the actin fine structure of the cytoskeleton (Figure 7). Indeed, it has been shown recently that TOC159, a major subunit of the chloroplast protein import complex involved in the import of photosynthesis proteins, directly interacts with actin (Bauer et al., 2000; Jouhet and Gray, 2009). Furthermore, there is a lot of evidence for interactions between actin and microtubule cytoskeleton via linking proteins (Petrásek and Schwarzerová, 2009). Another hypothesis is that the cytoskeleton is required not only for transport of proteins but also for transport of metabolites. More than one-third of the downregulated genes in *sco3-1* are involved in different metabolism pathways (lipids or carbohydrates) or are transporters. Metabolite transport deficiency has been shown to result in pale mesophyll cells as in the loss of the phosphoenolpyrovate/phosphate translocater PPT1 (Streatfield et al., 1999). Furthermore, the increased photoinhibition under extreme CO_2 conditions might indicate perturbed metabolite flux between the organelles. It may be that stromules participate in this interorganelle exchange of metabolites and/or proteins as they have been shown to alter protein exchange between plastids (Reski, 2009).

The finding that SCO3 is localized to the periphery of the peroxisome and not to chloroplasts, together with the observation that inhibiting the assembly of the microtubule cytoskeleton results in a loss of SCO3 localization, led us to assume that SCO3 is a microtubule-associated peroxisomal protein (Figure 8). Furthermore, the phenocopying of the *sco3-1* mutation with cytoskeleton inhibitors demonstrates that interactions between the plastid, cytoskeleton, and peroxisome are necessary for chloroplast and peroxisome biogenesis, morphology in cotyledons, and photosynthetic efficiency under altered CO_2 conditions in mature plants (Figure 8). The fact that knockouts of the SCO3 protein, which is unique to the plant kingdom, are lethal demonstrates that these and/or other functions of SCO3 are essential for the plant cell. Further insight into the function of SCO3 will be the subject of future research on the communication and the interaction between chloroplasts, peroxisomes, and the cytoskeleton. In conclusion, a previously uncharacterized protein, SCO3, is required for chloroplast biogenesis in seedlings, and the *sco3-1* mutation and microtubule inhibitors reveal a requirement for the cytoskeleton and peroxisomes in chloroplast biogenesis.

Table 2. Comparison of Chlorophyll Content of 5-d-Old Col Seedlings Treated with Actin (CD) or Tubulin (APM) Inhibitors

Inh.	Germ.	3 d Light → 2 d Inh.	3 d Dark→ 2 d Inh.
CD	81.7 ± 11	86.7 ± 11	70.5 ± 19
APM	64.9 ± 4	74.3 ± 15	56.0 ± 2

Chlorophyll content was measured in seedlings germinated for 5 d directly on inhibitor-containing media (Germ.) or for 3 d in normal MS media in the light or in the dark before being transferred to inhibitor-containing media and compared to untreated Col seedlings grown under the same growth conditions. The mean and SD are shown for two independent experiments with measurements taken from three independent samples. Inh., inhibitor applied to the sample.

METHODS

Plant Material and Growth Conditions

A screen on 75,000 pooled ethyl methylsulfonate–mutagenized seeds of *Arabidopsis thaliana* (ecotype Landsberg *erecta*) was performed in the M2 generation to search for mutants exhibiting pale cotyledons, but green true leaves (Albrecht et al., 2006) . To identify the *sco3-1* mutation, a map-based cloning approach was used in the F2 generation of a crossing with the Col ecotype. Since the phenotype of *sco3-1* is more pronounced in the Col background, further analyses have been performed with homozygous seedlings several times backcrossed into Col ecotype. Plants were grown under long-day conditions at 21°C on soil, or surface-sterilized seeds were plated on Murashige and Skoog (MS) media (Sigma-Aldrich) without sucrose. Transcript analyses with gene-specific primers on reverse-transcribed total RNA as well as pigment analysis from plant material harvested at the indicated time points have been performed as described (Albrecht et al., 2008).

Chloroplast Analyses

Chlorophyll measurement of embryos and seedlings was performed as described (Albrecht et al., 2008). Seven- and ten-day-old seedlings were used for chloroplast analysis under confocal laser scanning microscope (Leica) and transmission electron microscopy (TEM) analysis, respectively. For fixation and visualization of the ultrastructure of chloroplasts, cotyledons were incubated for 2 h in vacuum in primary fixation buffer (8.5 mL 0.1 M cacodylate buffer, 4% formaldehyde, and 0.5 mL glutaraldehyde). Following a washing step with cacodylate buffer (0.1 M, three times), the samples were incubated 1.5 h in 1% osmium-tetraoxide. After submitting the samples to a dehydration series in ascending concentration of ethanol, they were incubated in increasing concentrations of Epon Araldite. Finally, the samples were fixed in this resin at 65°C. Thin-layer cuttings were transferred on copper grids and stained 20 min with 5 to 6% uranium acetate and after washing with distilled water 15 min lead citrate. The washed and dried samples were analyzed using a TEM7100 Leica microscope.

The 77K Low Temperature Fluorescence measurements were performed as described (Albrecht et al., 2008) except that three 4 day old etiolated seedlings were used per measurement.

Generation of *SCO3* Constructs

The cDNA of the identified *SCO3* gene was cloned into the pENTR2B vector using primers containing *Sal*I and *Not*I restriction sites for in-frame cloning, respectively (see Supplemental Table 2 online). The correct insertion of the *SCO3* cDNA into the vector was verified by sequencing. Subsequently, this construct was used for cloning *SCO3* cDNA into the Gateway plant binary pMDC43 containing the 35S promoter (Curtis and Grossniklaus, 2003) for complementation analysis (GFP:SCO3). *sco3-1* mutant plants were transformed as described (Albrecht et al., 2008). In the same way, the cDNA of *Msco3-1* also was amplified and cloned into pMDC43 (GFP:Msco3-1) using mRNA of *sco3-1* as basis for cDNA synthesis. To verify that only the peroxisome-targeted SCO3 protein can complement *sco3-1*, *SCO3*-specific primers deleting the PTS1 at the C terminus were used to clone SCO3ΔSRL into the pENTR2B vector, with subsequent procedures of cloning into pMDC43 vector (GFP:SCO3ΔSRL) as described above (for primer information, see Supplemental Table 2 online). For localization analysis and targeting of SCO3 to the chloroplast, the *SCO3* cDNA was cloned into the pCAMBIA1302 vector (http://www.cambia.org/daisy/cambia/585.html) either without (SCO3:GFP) or with the chloroplast transit peptide of Rubisco small subunit (SSUcTP:SCO3:GFP). For the SSUcTP:SCO3:GFP construct, the nucleotides encoding the first 60 amino acids of Rubisco small subunit were amplified, ligated to the SCO3 cDNA, and the whole construct amplified with SSUcTP-NcoI-F and SCO3-NcoI-R. After digestion with *Nco*I, the fragment was cloned into pCAMBIA1302 and sequenced for control. The sequence-controlled construct was transformed into *sco3-1* mutant plants (for primer information, see Supplemental Table 2 online). Transformed plants were selected with the corresponding herbicide hygromycin. Localization studies and chloroplast import of the SCO3 protein were performed as described using vectors with either GFP fused to the whole SCO3 cDNA or the region encoding the first 100 amino acids of SCO3. These constructs were used to transform *Arabidopsis* cell culture or onion cells using a biolistic transformation protocol. Transformed cells were checked for GFP localization using confocal microscopy. The controls for localization, such as SSU:RFP and RFP:PTS1, have been described elsewhere (Carrie et al., 2009).

Identification and Characterization of T-DNA Insertion Lines

T-DNA express (http://signal.salk.edu/cgi-bin/tdnaexpress) was used to identify T-DNA insertion mutants of *SCO3*, and seeds of SALK lines were ordered from the ABRC (SALK_130239, *sco3-4*; SALK_065781, *sco3-2*; and SALK_09815, *sco3-3*). Plants of these T-DNA insertion lines were analyzed for the presence of the T-TNA using gene-specific primers as well as LB2 for the T-DNA insertion (for primer information, see Supplemental Table 2 online). The PCR products were sequenced to verify the insertion. To create the double mutant *sco3-1 phyB*, the *phyB-9* mutant was used (Reed et al., 1993).

Identification of the QWRF Protein Family

Using the SCO3 amino acid sequence, a BLASTX analysis was performed at the National Center for Biotechnology Information (http://www.ncbi.nlm.nih.gov/) to identify other proteins similar to SCO3. A ClustalW analysis (http://www.ebi.ac.uk/Tools/clustalw2/index.html) was conducted using the provided amino acid sequences at the accessions listed in Supplemental Figure 3 online.

Gene Expression Analysis

Total mRNA of *sco3*-1 and Col was isolated, DNase treated, and reverse transcribed, and RT-PCR analysis was performed as described and compared with the 18SrRNA expression (Albrecht et al., 2006). Transcript profiling of the plastid transcriptome was performed using the same primers for the quantitative PCR approach as described (Delannoy et al., 2009). The Norflurazon treatment of *sco3-1* was performed as described for the *gun* mutants (Koussevitzky et al., 2007). For transcriptome analysis using GeneChip *Arabidopsis* Genome ATH1 arrays, mRNA of 4-d-old seedlings of *sco3-1* and Col were isolated and prepared as described (Cazzonelli et al., 2009). The obtained CEL files were further analyzed in GeneSpring GX10 (Agilent) using first GC-RMA for raw intensity data normalization. Scatterplots showed a high correlation for all three replicates per plant line of between 0.986 and 0.996 for Col samples and 0.987 and 0.994 for *sco3-1* samples. The log-transformed data were subsequently analyzed for differential expression of genes between *sco3-1* and Col using the unpaired *t* test with an asymptotic P value computation, a permutation of 100, and a multiple testing correction using Benjamin Hochberg false discovery rate (level used of 0.05). Genes with a differential expression of more than twofold were selected and further analyzed. A hierarchical analysis of the obtained genes was performed. The examination of present/absent genes was performed in a similar way using MAS5 for raw intensity data normalization on a baseline to media of samples. Genes with a differential expression more than twofold were further analyzed. Identified genes were subsequently introduced for analysis into the MapMan databases (http://www.gabipd.org/projects/MapMan/) to search for changed metabolic pathways or processes. The

same genes were also submitted into the Genevestigator databases (https://www.genevestigator.com/gv/index.jsp) and compared with expression data from *gun1-9*, *gun5*, and Col treated with Norflurazon (Koussevitzky et al., 2007). The accession number of the array data obtained for *sco3-1*/wild type is Albrecht_SCO3 and is in the publically available database of ArrayExpress (http://www.ebi.ac.uk/arrayexpress/).

Protein Analysis

Total protein was extracted from 4-d-old seedlings as described (Albrecht et al., 2006). Then, 15 μg of protein was separated on SDS gels and either stained with Coomassie Brilliant Blue for loading controls or used for immunoblot analysis with LHCB2 primary antibody (Agrisera) and goat-anti-chicken secondary antibody (Pierce). Fluorescence was detected using the SuperSignal West Pico Chemiluminescent Substrate from Thermo-Science.

β-Oxidation Analysis

Since the root growth in *sco3-1* is quite heterogeneous, the hypocotyl lengths of 4-d-old etiolated seedlings grown on MS media without sucrose but containing 0, 5, 10, 15, or 20 μM IBA (Sigma) were measured and compared with the hypocotyl lengths at 0 μM IBA (which were calculated as 100%). IBA gets β-oxidized in the peroxisomes to the plant hormone auxin, resulting in reduced hypocotyl growth (Poupart et al., 2005).

Photorespiration Analysis

It has recently been shown that impaired photorespiration may be readily detected in mutants by the fact that when plants are exposed to low CO_2 in the light there is rapid net damage to PSII leading to a decline in the dark adapted F_v/F_m chlorophyll fluorescence parameter associated with PSII function (Takahashi et al., 2007). To examine this in *sco3-1* mutants, seedlings were grown for 7 and 14 d under high CO_2 concentrations (0.6% CO_2), transferred for 24 h to 0% CO_2 or to air (ambient CO_2) in continuous light, and dark adapted F_v/F_m measured with a chlorophyll fluorescence imaging device (PAM; Waltz) both before and after the transfer.

Plants of *sco3-1* and Col were grown under high CO_2 (0.6%) at short-day conditions at moderate light of 150 μm/s m^2 to compare growth of mature plants.

Cytoskeleton Inhibitor Application

To investigate if the cytoskeleton is required for chloroplast development, we used inhibitors for actin (CD) and microtubules (APM). MS media containing either 40 μM CD for actin inhibition or 10 μM APM for microtubule inhibition were used. Surface-sterilized seeds were either plated directly on the inhibitor-containing MS plates for 5 d or on normal MS media for 3-d-old seedling grown on MS media either in the dark or under light before being transferred on inhibitor-containing MS plates and further exposed to light for two more days.

Transient Seedling Transformation

Transient seedling transformation was performed using 5 mL agrobacteria pelleted and resuspended in 10 mL infiltration media on 4-d-old seedlings. After 10-min incubation, the seedlings were washed three times with infiltration media. Transformed cells expressing GFP-fused talin for visualizing actin were analyzed 3 d later under the confocal laser scanning microscope (Leica) (Takemoto et al., 2003).

Phylogenetic Analysis

For the phylogenetic analysis, the program Mega4.0.2 was used. The protein sequences have been downloaded from the National Center for Biotechnology Information (http://www.ncbi.nlm.nih.gov/) or Uniprot (http://www.uniprot.org/) and aligned using the ClustalW method in Mega 4 (pairwise alignment: gap opening penalty 10, gap extension penalty 0.1; multiple alignment: gap opening penalty 10, gap extension penalty 0.2, protein weight matrix using Gonnet). The residue-specific and hydrophilic penalties were ON, whereas the End Gap separation and the Use negative separation was OFF. Gap separation distance used was 4, and the delay divergence cutoff was at 30. This checked alignment (available as Supplemental Data Set 2 online) was then used for a bootstrap test (1000 replicates, seed = 86,477) for phylogeny using the neighbor-joining method (Poisson correction, a complete deletion of the gaps). Shown is the bootstrap consensus tree in Supplemental Figure 9 online.

Accession Numbers

Sequence data from this article can be found in the Arabidopsis Genome Initiative or GenBank/EMBL databases under the following accession numbers: SCO3/QWRF1, At3g19570; QWRF2, At1g49890; QWRF3, At2g20815; QWRF4, At2g24070; QWRF5/EDE1, At2g44190; QWRF6, At3g60000; QWRF7, At4g25190; QWRF8, At4g30710; and QWRF9, At5g43160. Furthermore, the protein data used for the QWRF protein family analysis are of the following proteins of other plant species: A7NU78, A7QL53, A7PFN8, A5AUO2, H5ASP7, A7QAR3, Q6K675, Q69P50, Q9AV13, Q75ID9, Q94HE4, Q339L2, Q6EN70, Q339L1, Q8H2N8, Q8W5H2, Q339L3, Q1EPE9, A9SPE9, A9TVI0, A9U2E5, and A9TVC6. Genes used for transcript analysis are as follows: LHCB1.2, At1g29920; LHCB1.5, At2g34420; LHCB2.4, AT3G27690; PORB, At4g27440; and rbcS/SSU, At1g67090. The accession number of the array data obtained for *sco3-1*/wild type is Albrecht_SCO3 in the publically available database of ArrayExpress (http://www.ebi.ac.uk/arrayexpress/).

Supplemental Data

The following materials are available in the online version of this article.

Supplemental Figure 1. Embryo Development in the *sco3-1* Mutant.

Supplemental Figure 2. Measurement of the Protochlorophyllide Autofluorescence in 4-d-Old Etiolated Seedlings of *sco3-1*.

Supplemental Figure 3. Quantitative Real-Time PCR Analysis of Transcript Levels of Chloroplast-Encoded Genes.

Supplemental Figure 4. RT-PCR Analysis of Transcript Levels of Retrograde Signaling-Controlled Nuclear Genes in *sco3-1* and Col on Norflurazon.

Supplemental Figure 5. Microarray Analysis.

Supplemental Figure 6. MapMan Analysis Showing Down- and Upregulated Genes in *sco3-1.*

Supplemental Figure 7. Hierarchical Graph of the Expression Data of Differentially Expressed Genes in Col and *sco3-1*.

Supplemental Figure 8. The Identification of the *SCO3* Gene.

Supplemental Figure 9. Phylogenetic Tree of the ClustalW Analysis of the Identified QWRF Proteins in *Arabidopsis thaliana*, *Oryza sativa*, *Musa accuminata*, and *Physcomitrella patens.*

Supplemental Figure 10. ClustalW Alignment of the QWRF Domain of the Different QWRF Proteins in *Arabidopsis thaliana*.

Supplemental Figure 11. Immunoblot Analysis on Total Protein of 4-d-Old Seedlings of Col, *sco3-1*, *phyB*, and *sco3-1 phyB* Using Monoclonal LHCB2 Antibody.

Supplemental Table 1. List of the Identified QWRF Proteins in Different Plant Species.

Supplemental Table 2. Primers Used for the Different Analyses.

Supplemental Movie 1. GFP:SCO3 Localization in an Onion Cell.

Supplemental Data Set 1. Microarray Data from Transcript Analysis of *sco3-1* and Col of 4-d-Old Seedlings.

Supplemental Data Set 2. Text File of the Alignment Used for Generating the Phylogenetic Tree in Supplemental Figure 9 Online.

ACKNOWLEDGMENTS

We thank Lily Shen from the electron microscopy unit, Australian National University Canberra, who helped with preparation of TEM samples, and Dierk Wanke and Joachim Kilian (Zentrum für Molekularbiologie der Pflanzen Tubingen), who helped with coregulated gene expression analyses. We also thank Brian Gunning for the help in interpreting the TEM pictures. The talin:GFP construct was generously provided by Adrienne Hardham and the cpTP:GFP by Spencer Whitney, Australian National University Canberra. This project received support from the Australian Research Council Centre of Excellence in Plant Energy Biology (CE0561495).

Received February 16, 2010; revised August 22, 2010; accepted October 6, 2010; published October 26, 2010.

REFERENCES

Albrecht, V., Ingenfeld, A., and Apel, K. (2006). Characterization of the snowy cotyledon 1 mutant of *Arabidopsis thaliana*: The impact of chloroplast elongation factor G on chloroplast development and plant vitality. Plant Mol. Biol. **60:** 507–518.

Albrecht, V., Ingenfeld, A., and Apel, K. (2008). Snowy cotyledon 2: The identification of a zinc finger domain protein essential for chloroplast development in cotyledons but not in true leaves. Plant Mol. Biol. **66:** 599–608.

Apuya, N.R., Yadegari, R., Fischer, R.L., Harada, J.J., Zimmerman, J.L., and Goldberg, R.B. (2001). The Arabidopsis embryo mutant schlepperless has a defect in the chaperonin-60alpha gene. Plant Physiol. **126:** 717–730.

Asano, T., Yoshioka, Y., and Machida, Y. (2004). A defect in atToc159 of *Arabidopsis thaliana* causes severe defects in leaf development. Genes Genet. Syst. **79:** 207–212.

Bauer, J., Chen, K., Hiltbunner, A., Wehrli, E., Eugster, M., Schnell, D., and Kessler, F. (2000). The major protein import receptor of plastids is essential for chloroplast biogenesis. Nature **403:** 203–207.

Buchner, O., Holzinger, A., and Lütz, C. (2007). Effects of temperature and light on the formation of chloroplast protrusions in leaf mesophyll cells of high alpine plants. Plant Cell Environ. **30:** 1347–1356.

Carrie, C., Kühn, K., Murcha, M.W., Duncan, O., Small, I.D., O'Toole, N., and Whelan, J. (2009). Approaches to defining dual-targeted proteins in Arabidopsis. Plant J. **57:** 1128–1139.

Castillon, A., Shen, H., and Huq, E. (2007). Phytochrome Interacting Factors: Central players in phytochrome-mediated light signaling networks. Trends Plant Sci. **12:** 514–521.

Cazzonelli, C.I., Cuttriss, A.J., Cossetto, S.B., Pye, W., Crisp, P., Whelan, J., Finnegan, E.J., Turnbull, C., and Pogson, B.J. (2009). Regulation of carotenoid composition and shoot branching in *Arabidopsis* by a chromatin modifying histone methyltransferase, SDG8. Plant Cell **21:** 39–53.

Chen, M., Choi, Y., Voytas, D.F., and Rodermel, S. (2000). Mutations in the Arabidopsis VAR2 locus cause leaf variegation due to the loss of a chloroplast FtsH protease. Plant J. **22:** 303–313.

Chory, J. (1991). Light signals in leaf and chloroplast development: photoreceptors and downstream responses in search of a transduction pathway. New Biol. **3:** 538–548.

Curtis, M.D., and Grossniklaus, U. (2003). A gateway cloning vector set for high-throughput functional analysis of genes in planta. Plant Physiol. **133:** 462–469.

Delannoy, E., Le Ret, M., Faivre-Nitschke, E., Estavillo, G.M., Bergdoll, M., Taylor, N.L., Pogson, B.J., Small, I., Imbault, P., and Gualberto, J.M. (2009). *Arabidopsis* tRNA adenosine deaminase arginine edits the wobble nucleotide of chloroplast tRNAArg(ACG) and is essential for efficient chloroplast translation. Plant Cell **21:** 2058–2071.

Foyer, C.H., Bloom, A.J., Queval, G., and Noctor, G. (2009). Photorespiratory metabolism: Genes, mutants, energetics, and redox signaling. Annu. Rev. Plant Biol. **60:** 455–484.

Glynn, J.M., Miyagishima, S.Y., Yoder, D.W., Osteryoung, K.W., and Vitha, S. (2007). Chloroplast division. Traffic **8:** 451–461.

Gunning, B.E. (1965). The fine structure of chloroplast stroma following aldehyde osmium-tetroxide fixation. J. Cell Biol. **24:** 79–93.

Gunning, B.E. (2005). Plastid stromules: Video microscopy of their outgrowth, retraction, tensioning, anchoring, branching, bridging, and tip-shedding. Protoplasma **225:** 33–42.

Gutensohn, M., et al. (2004). Characterization of a T-DNA insertion mutant for the protein import receptor atToc33 from chloroplasts. Mol. Genet. Genomics **272:** 379–396.

Hardham, A.R., Takemoto, D., and White, R.G. (2008). Rapid and dynamic subcellular reorganization following mechanical stimulation of Arabidopsis epidermal cells mimics responses to fungal and oomycete attack. BMC Plant Biol. **8:** 63.

Heazlewood, J.L., Verboom, R.E., Tonti-Filippini, J., Small, I., and Millar, A.H. (2007). SUBA: The Arabidopsis Subcellular Database. Nucleic Acids Res. **35**(Database issue): D213–D218.

Holzinger, A., Buchner, O., Lütz, C., and Hanson, M.R. (2007). Temperature-sensitive formation of chloroplast protrusions and stromules in mesophyll cells of *Arabidopsis thaliana*. Protoplasma **230:** 23–30.

Hu, J., Aguirre, M., Peto, C., Alonso, J., Ecker, J., and Chory, J. (2002). A role for peroxisomes in photomorphogenesis and development of Arabidopsis. Science **297:** 405–409.

Inoue, K., Baldwin, A.J., Shipman, R.L., Matsui, K., Theg, S.M., and Ohme-Takagi, M. (2005). Complete maturation of the plastid protein translocation channel requires a type I signal peptidase. J. Cell Biol. **171:** 425–430.

Ishida, H., Yoshimoto, K., Izumi, M., Reisen, D., Yano, Y., Makino, A., Ohsumi, Y., Hanson, M.R., and Mae, T. (2008). Mobilization of rubisco and stroma-localized fluorescent proteins of chloroplasts to the vacuole by an ATG gene-dependent autophagic process. Plant Physiol. **148:** 142–155.

Ishizaki, Y., Tsunoyama, Y., Hatano, K., Ando, K., Kato, K., Shinmyo, A., Kobori, M., Takeba, G., Nakahira, Y., and Shiina, T. (2005). A nuclear-encoded sigma factor, Arabidopsis SIG6, recognizes sigma-70 type chloroplast promoters and regulates early chloroplast development in cotyledons. Plant J. **42:** 133–144.

Jouhet, J., and Gray, J.C. (2009). Interaction of actin and the chloroplast protein import apparatus. J. Biol. Chem. **284:** 19132–19141.

Kadota, A., Yamada, N., Suetsugu, N., Hirose, M., Saito, C., Shoda, K., Ichikawa, S., Kagawa, T., Nakano, A., and Wada, M. (2009). Short actin-based mechanism for light-directed chloroplast movement in Arabidopsis. Proc. Natl. Acad. Sci. USA **106:** 13106–13111.

Ketelaar, T., Voss, C., Dimmock, S.A., Thumm, M., and Hussey, P.J.

(2004). Arabidopsis homologues of the autophagy protein Atg8 are a novel family of microtubule binding proteins. FEBS Lett. **567:** 302–306.

Koussevitzky, S., Nott, A., Mockler, T.C., Hong, F., Sachetto-Martins, G., Surpin, M., Lim, J., Mittler, R., and Chory, J. (2007). Signals from chloroplasts converge to regulate nuclear gene expression. Science **316:** 715–719.

Kwok, E.Y., and Hanson, M.R. (2003). Microfilaments and microtubules control the morphology and movement of non-green plastids and stromules in *Nicotiana tabacum*. Plant J. **35:** 16–26.

Lopez-Juez, E., and Pyke, K.A. (2005). Plastids unleashed: Their development and their integration in plant development. Int. J. Dev. Biol. **49:** 557–577.

Lütz, C., and Engel, L. (2007). Changes in chloroplast ultrastructure in some high-alpine plants: Adaptation to metabolic demands and climate? Protoplasma **231:** 183–192.

Marrison, J.L., Rutherford, S.M., Robertson, E.J., Lister, C., Dean, C., and Leech, R.M. (1999). The distinctive roles of five different ARC genes in the chloroplast division process in Arabidopsis. Plant J. **18:** 651–662.

Miura, E., Kato, Y., Matsushima, R., Albrecht, V., Laalami, S., and Sakamoto, W. (2007). The balance between protein synthesis and degradation in chloroplasts determines leaf variegation in *Arabidopsis* yellow variegated mutants. Plant Cell **19:** 1313–1328.

Monte, E., Tepperman, J.M., Al-Sady, B., Kaczorowski, K.A., Alonso, J.M., Ecker, J.R., Li, X., Zhang, Y., and Quail, P.H. (2004). The phytochrome-interacting transcription factor, PIF3, acts early, selectively, and positively in light-induced chloroplast development. Proc. Natl. Acad. Sci. USA **101:** 16091–16098.

Moon, J., Zhu, L., Shen, H., and Huq, E. (2008). PIF1 directly and indirectly regulates chlorophyll biosynthesis to optimize the greening process in Arabidopsis. Proc. Natl. Acad. Sci. USA **105:** 9433–9438.

Natesan, S.K., Sullivan, J.A., and Gray, J.C. (2005). Stromules: a characteristic cell-specific feature of plastid morphology. J. Exp. Bot. **56:** 787–797.

Natesan, S.K., Sullivan, J.A., and Gray, J.C. (2009). Myosin XI is required for actin-associated movement of plastid stromules. Mol. Plant **2:** 1262–1272.

Olmos, E., Kiddle, G., Pellny, T., Kumar, S., and Foyer, Ch. (2006). Modulation of plant morphology, root architecture, and cell structure by low vitamin C in *Arabidopsis thaliana*. J. Exp. Bot. **57:** 1645–1655.

Oswald, O., Martin, T., Dominy, P.J., and Graham, I.A. (2001). Plastid redox state and sugars: Interactive regulators of nuclear-encoded photosynthetic gene expression. Proc. Natl. Acad. Sci. USA **98:** 2047–2052.

Petrásek, J., and Schwarzerová, K. (2009). Actin and microtubule cytoskeleton interactions. Curr. Opin. Plant Biol. **12:** 728–734.

Pignocchi, C., Minns, G.E., Nesi, N., Koumproglou, R., Kitsios, G., Benning, C., Lloyd, C.W., Doonan, J.H., and Hills, M.J. (2009). ENDOSPERM DEFECTIVE1 is a novel microtubule-associated protein essential for seed development in *Arabidopsis*. Plant Cell **21:** 90–105.

Pogson, B.J., Woo, N.S., Förster, B., and Small, I.D. (2008). Plastid signalling to the nucleus and beyond. Trends Plant Sci. **13:** 602–609.

Poupart, J., Rashotte, A.M., Muday, G.K., and Waddell, C.S. (2005). The rib1 mutant of Arabidopsis has alterations in indole-3-butyric acid transport, hypocotyl elongation, and root architecture. Plant Physiol. **139:** 1460–1471.

Reed, J.W., Nagpal, P., Poole, D.S., Furuya, M., and Chory, J. (1993). Mutations in the gene for the red/far-red light receptor phytochrome B alter cell elongation and physiological responses throughout *Arabidopsis* development. Plant Cell **5:** 147–157.

Reski, R. (2009). Challenges to our current view on chloroplasts. Biol. Chem. **390:** 731–738.

Reumann, S. (2004). Specification of the peroxisome targeting signals type 1 and type 2 of plant peroxisomes by bioinformatics analyses. Plant Physiol. **135:** 783–800.

Schumann, U., Prestele, J., O'Geen, H., Brueggeman, R., Wanner, G., and Gietl, C. (2007). Requirement of the C3HC4 zinc RING finger of the Arabidopsis PEX10 for photorespiration and leaf peroxisome contact with chloroplasts. Proc. Natl. Acad. Sci. USA **104:** 1069–1074.

Sheahan, M.B., Rose, R.J., and McCurdy, D.W. (2004). Organelle inheritance in plant cell division: The actin cytoskeleton is required for unbiased inheritance of chloroplasts, mitochondria and endoplasmic reticulum in dividing protoplasts. Plant J. **37:** 379–390.

Shimada, H., Mochizuki, M., Ogura, K., Froehlich, J.E., Osteryoung, K.W., Shirano, Y., Shibata, D., Masuda, S., Mori, K., and Takamiya, K. (2007). *Arabidopsis* cotyledon-specific chloroplast biogenesis factor CYO1 is a protein disulfide isomerase. Plant Cell **19:** 3157–3169.

Sinclair, A.M., Trobacher, C.P., Mathur, N., Greenwood, J.S., and Mathur, J. (2009). Peroxule extension over ER-defined paths constitutes a rapid subcellular response to hydroxyl stress. Plant J. **59:** 231–242.

Slavikova, S., Ufaz, S., Avin-Wittenberg, T., Levanony, H., and Galili, G. (2008). An autophagy-associated Atg8 protein is involved in the responses of Arabidopsis seedlings to hormonal controls and abiotic stresses. J. Exp. Bot. **59:** 4029–4043.

Somers, D.E., Sharrock, R.A., Tepperman, J.M., and Quail, P.H. (1991). The hy3 long hypocotyl mutant of *Arabidopsis* is deficient in phytochrome B. Plant Cell **3:** 1263–1274.

Sorek, N., Bloch, D., and Yalovsky, S. (2009). Protein lipid modifications in signaling and subcellular targeting. Curr. Opin. Plant Biol. **12:** 714–720.

Stephenson, P.G., Fankhauser, C., and Terry, M.J. (2009). PIF3 is a repressor of chloroplast development. Proc. Natl. Acad. Sci. USA **106:** 7654–7659.

Streatfield, S.J., Weber, A., Kinsman, E.A., Häusler, R.E., Li, J., Post-Beittenmiller, D., Kaiser, W.M., Pyke, K.A., Flügge, U.I., and Chory, J. (1999). The phosphoenolpyruvate/phosphate translocator is required for phenolic metabolism, palisade cell development, and plastid-dependent nuclear gene expression. Plant Cell **11:** 1609–1622.

Surpin, M., Larkin, R.M., and Chory, J. (2002). Signal transduction between the chloroplast and the nucleus. Plant Cell **14**(Suppl): S327–S338.

Takahashi, S., Bauwe, H., and Badger, M. (2007). Impairment of the photorespiratory pathway accelerates photoinhibition of photosystem II by suppression of repair but not acceleration of damage processes in Arabidopsis. Plant Physiol. **144:** 487–494.

Takemoto, D., Jones, D.A., and Hardham, A.R. (2003). GFP-tagging of cell components reveals the dynamics of subcellular re-organization in response to infection of Arabidopsis by oomycete pathogens. Plant J. **33:** 775–792.

Vinti, G., Hills, A., Campbell, S., Bowyer, J.R., Mochizuki, N., Chory, J., and López-Juez, E. (2000). Interactions between hy1 and gun mutants of Arabidopsis, and their implications for plastid/nuclear signalling. Plant J. **24:** 883–894.

Waters, M.T., Wang, P., Korkaric, M., Capper, R.G., Saunders, N.J., and Langdale, J.A. (2009). GLK transcription factors coordinate expression of the photosynthetic apparatus in *Arabidopsis*. Plant Cell **21:** 1109–1128.

Woo, N.S., Badger, M.R., and Pogson, B.J. (2008). A rapid, non-invasive procedure for quantitative assessment of drought survival using chlorophyll fluorescence. Plant Methods **4:** 27.

Yamamoto, Y.Y., Puente, P., and Deng, X.W. (2000). An Arabidopsis cotyledon-specific albino locus: A possible role in 16S rRNA maturation. Plant Cell Physiol. **41:** 68–76.